Journal of Zhejiang University-SCIENCE B (Biomedicine & Biotechnology) 2023 24(1):32-49
www.jzus.zju.edu.cn; www.springer.com/journal/11585
E-mail: jzus_b@zju.edu.cn

Research Article

https://doi.org/10.1631/jzus.B2200269

Hypoxia-induced ROS aggravate tumor progression through HIF-1α-SERPINE1 signaling in glioblastoma

Lin ZHANG[1,2*], Yuanyuan CAO[2,3*], Xiaoxiao GUO[2,4], Xiaoyu WANG[2], Xiao HAN[5], Kouminin KANWORE[2], Xiaoliang HONG[2], Han ZHOU[2], Dianshuai GAO[2✉]

[1]*School of Nursing, Xuzhou Medical University, Xuzhou 221004, China*
[2]*Department of Neurobiology and Anatomy, Xuzhou Key Laboratory of Neurobiology, Xuzhou Medical University, Xuzhou 221004, China*
[3]*Department of Ultrasound, Taizhou Hospital of Traditional Chinese Medicine, Taizhou 225300, China*
[4]*Department of Basic Medicine, Kangda College of Nanjing Medical University, Lianyungang 222000, China*
[5]*The Fourth School of Medicine, Nanjing Medical University, Nanjing 211166, China*

Abstract: Hypoxia, as an important hallmark of the tumor microenvironment, is a major cause of oxidative stress and plays a central role in various malignant tumors, including glioblastoma. Elevated reactive oxygen species (ROS) in a hypoxic microenvironment promote glioblastoma progression; however, the underlying mechanism has not been clarified. Herein, we found that hypoxia promoted ROS production, and the proliferation, migration, and invasion of glioblastoma cells, while this promotion was restrained by ROS scavengers *N*-acetyl-L-cysteine (NAC) and diphenyleneiodonium chloride (DPI). Hypoxia-induced ROS activated hypoxia-inducible factor-1α (HIF-1α) signaling, which enhanced cell migration and invasion by epithelial-mesenchymal transition (EMT). Furthermore, the induction of serine protease inhibitor family E member 1 (SERPINE1) was ROS-dependent under hypoxia, and HIF-1α mediated SERPINE1 increase induced by ROS via binding to the *SERPINE1* promoter region, thereby facilitating glioblastoma migration and invasion. Taken together, our data revealed that hypoxia-induced ROS reinforce the hypoxic adaptation of glioblastoma by driving the HIF-1α-SERPINE1 signaling pathway, and that targeting ROS may be a promising therapeutic strategy for glioblastoma.

Key words: Glioblastoma; Hypoxia; Reactive oxygen species (ROS); Hypoxia-inducible factor-1α (HIF-1α); Serine protease inhibitor family E member 1 (SERPINE1)

1 Introduction

Glioblastoma (GBM) is the most common aggressive primary brain tumor. Although therapeutic strategies have advanced in recent years, the median survival time of GBM patients is less than 15 months even after surgical resection and adjuvant therapy (Omuro and DeAngelis, 2013; Olar and Aldape, 2014). Hypoxia is widely considered as a crucial feature of the tumor microenvironment (TME) (Wilson and Hay, 2011), including the TME in GBM (Vordermark, 2005; Srivastava et al., 2018). The adaptation of GBM cells to hypoxic conditions is a key driving force leading to chemoradiotherapy resistance and a malignant phenotype (Kessler et al., 2010; Jin et al., 2018; Wang et al., 2021). Therefore, it is essential to elucidate the molecular mechanisms of tumor adaptation to hypoxia. Recent studies have uncovered that hypoxia stimulates reactive oxygen species (ROS) generation (Dabral et al., 2019; Yu et al., 2019; Zong et al., 2020). Moderate ROS are important in biological processes under physiological conditions. Nonetheless, tumor cells produce higher ROS resulting from aberrant metabolism compared with normal cells. Notably, because of the dual nature of ROS, their moderate elevation promotes cancer progression, whereas their extreme accumulation drives cancer cell death (Perillo et al., 2020). However, the exact levels and functions of ROS in hypoxic GBM remain elusive.

Hypoxia-inducible factor-1 (HIF-1) is a well-recognized, central transcription factor in cellular

✉ Dianshuai GAO, gds@xzhmu.edu.cn
* The two authors contributed equally to this work
Dianshuai GAO, https://orcid.org/0000-0001-8567-0238

Received May 10, 2022; Revision accepted July 28, 2022;
Crosschecked Jan. 10, 2023

adaptation to hypoxia (Harris, 2002; Semenza, 2014). HIF-1 is composed of a constitutive β-subunit (HIF-1β) and an oxygen-sensitive α-subunit (HIF-1α). In normoxia, the level of HIF-1α is low due to proteasomal degradation mediated by von Hippel-Lindau (VHL) protein. Meanwhile, in hypoxia, the interaction between HIF-1α and VHL is inhibited, contributing to HIF-1α stabilization and nuclear accumulation. Recent evidence has shown the promoting effects of ROS on the stability and activation of HIF-1α (Schumacker, 2011; Dabral et al., 2019; Sun et al., 2021; Willson et al., 2022), which subsequently transactivates numerous genes to augment hypoxic adaptation (Semenza, 1998; Ke and Costa, 2006; Fandrey and Gassmann, 2009) via binding to the hypoxia response elements (HREs) of target genes. Considering the importance of HIF-1α in cancer progression (Zhao et al., 2023), we speculate that hypoxia-induced ROS may regulate downstream gene expression via activating the HIF-1α pathway to facilitate GBM growth.

Serine protease inhibitor family E member 1 (SERPINE1, or plasminogen activator inhibitor-1 (PAI-1)) is the major inhibitor of urokinase plasminogen activator (uPA) system and is originally considered as a cancer suppressor. Conversely, SERPINE1 is abnormally expressed in various cancers and correlated with tumor progression (Takayama et al., 2016; Li et al., 2019; Teng et al., 2021). Emerging research has revealed an association between aberrant SERPINE1 expression and strong invasiveness as well as poor prognosis in GBM (Wang et al., 2020). Although SERPINE1 was reported to be upregulated under hypoxic conditions in GBM (Chédeville et al., 2020), whether it is involved in GBM progression induced by hypoxia remains unknown. Earlier studies have found that HIF-1α mediates its transcription by directly binding to the *SERPINE1* promoter (Andrew et al., 2001; Fink et al., 2002). Therefore, the ROS-HIF-1α-SERPINE1 axis may promote the adaptation of GBM cells to hypoxia.

This work was aimed to investigate the molecular mechanism of the adaptation to hypoxia in GBM. First, we assessed the levels and functions of ROS in GBM cells under hypoxia. Next, we determined the effect of ROS in HIF-1α activation and whether ROS functions were dependent on HIF-1α. Finally, the downstream mechanism by ROS-HIF-1α was explored. Taken together, our work indicated that the ROS-HIF-1α-SERPINE1 pathway plays a vital role in GBM adaptation to hypoxia, providing new evidence for ROS as a potential target for GBM treatment.

2 Materials and methods

2.1 Cell lines and culture conditions

Human GBM cell lines (U87, U251, and LN229) were obtained from the American Type Culture Collection (ATCC; Rockville, MD, USA) and authenticated by short tandem repeat (STR) profiling. The HEK293T cell line was purchased from the Cell Bank of Chinese Academy of Sciences (Shanghai, China). All cell lines were incubated in Dulbecco's modified Eagle's medium (DMEM; Hyclone, Utah, USA) supplemented with 10% (0.1 g/mL) fetal bovine serum (FBS; Gibco, Grand Island, NY, USA) in 5% CO_2 at 37 °C. For the hypoxia groups, 24 h post-seeding, the cells were cultured with new medium that had been pre-treated in a hypoxia incubator (Thermo, Waltham, MA, USA) under 1% O_2/5% CO_2 conditions for 4 h, and they were exposed to hypoxic environments for the indicated time periods. For the normoxia groups, the cells were maintained in 21% O_2/5% CO_2 for the matching time periods.

In this study, U87 and U251 cells were frequently subjected to ROS inhibitors, including *N*-acetyl-L-cysteine (NAC; MedChemExpress, Monmouth Junction, NJ, USA) and diphenyleneiodonium chloride (DPI; MedChemExpress). For the inhibitor intervention experiment, U87 and U251 cells were pre-treated by NAC (1 or 5 mmol/L) or DPI (5 or 10 μmol/L) reagents for 4 h under normoxic conditions before hypoxia exposure as described above.

2.2 qPCR

Total RNA was extracted using TRIzol reagents (Vazyme, Nanjing, China), and then reversely transcribed into complementary DNA (cDNA) using the Hifair® II 1st Strand cDNA Synthesis Kit (YEASEN, Shanghai, China). Quantitative real-time polymerase chain reaction (qPCR) was performed using the Hieff® qPCR SYBR Green Master Mix (YEASEN) following the manufacturer's instructions. Each experiment was carried out in triplicate and repeated three times. *β-Actin* was used as a reference gene. The $2^{-\Delta\Delta C_T}$ method was applied to calculate the relative expression levels

of target genes. The qPCR primer sequences are listed in Table S1.

2.3 Western blotting and antibodies

Total and nuclear proteins were extracted from cell lysates using total protein (Biosharp, Guangzhou, China) and nuclear protein extraction reagents (Beyotime, Shanghai, China), respectively. Protein samples were analyzed by western blotting using standard procedures. Briefly, protein extracts were separated by sodium dodecyl sulfate-polyacrylamide gel electrophoresis (SDS-PAGE), transferred to polyvinylidene fluoride (PVDF) membranes (Millipore, Boston, MA, USA), and blocked with 5% (0.05 g/mL) skimmed milk in Tris-buffered saline with Tween-20 (TBST) for 2 h. The membranes were incubated with the primary antibodies overnight at 4 ℃, and then with the secondary antibodies at room temperature for 1 h. The visible bands were scanned by ChemiDoc XRS+ (BioRad, Hercules, CA, USA), and quantified by ImageJ software (Version 6, NIMH, Bethesda, MD, USA). β-Actin and Lamina A/C were used as the loading controls of total protein and nuclear protein, respectively. The antibodies used are shown in Table S2.

2.4 ELISA

Extracellular SERPINE1 levels were assessed using a human SERPINE1 enzyme-linked immunosorbent assay (ELISA) Kit (USCNK, Wuhan, China) according to the manufacturer's recommendations. Briefly, cell supernatants were collected and standards were added to sample wells and standard wells, respectively. All wells except the blank well were incubated in 100 μL enzyme conjugate for 1 h at 37 ℃, and then washed five times. Subsequently, each well was incubated with 100 μL Substrate A for 1 h at 37 ℃ and then added with 100 μL Substrate B for 30 min at 37 ℃. After 50 μL stop solution was added to each well, the optical density values at 450 nm (OD_{450}) were obtained within 15 min using a microplate reader (Molecular Devices, I3, Silicon, CA, USA).

2.5 Immunofluorescence

U251 and U87 cells grown on coverslips in 24-well plates were fixed with 4% (volume fraction) paraformaldehyde for 30 min and permeabilized with 1% (volume fraction) Triton X-100 for 10 min. After blocking for 30 min using 5% (0.05 g/mL) bovine serum albumin (BSA; TaKaRa, Tokyo, Japan), cells were incubated in rabbit anti-HIF-1α antibody (#AF1009; Affinity, Cincinnati, OH, USA) diluted in phosphate-buffered saline (PBS) overnight at 4 ℃. Then, cells were incubated with a secondary antibody fluorescein isothiocyanate (FITC; Biosharp) for 2 h at 37 ℃. The nuclei were stained with Hoechst (Beyotime). Fluorescence images were captured under a confocal microscope (STELLARIS 5, Leica, Wetzlar, Germany) at the same exposure intensity.

2.6 ROS measurement

ROS levels were detected by the ROS Assay Kit (Beyotime) according to the protocols (https://www.beyotime.com/mobilegoods.do?method=code&code=S0033S). Cells were rinsed with PBS and then incubated with 10 μmol/L 2',7'-dichlorodihydrofluorescein-diacetate (DCFH-DA) for 20 min at 37 ℃ in a hypoxia incubator. After washing with serum-free medium three times to remove extracellular DCFH-DA, cells were analyzed using a flow cytometer (LSRFortessa, BD, San Jose, CA, USA) or imaged by fluorescence microscope (Olympus, Tokyo, Japan). The fluorescence images were quantified by ImageJ software.

2.7 Cell viability assay

Cell counting kit-8 (CCK-8) assay was performed to measure the cell viability. U251 and U87 cells were grown in 96-well plates overnight, and then exposed to the indicated treatments for 24 or 48 h. After adding CCK-8 reagent (Dojindo, Kumamoto, Japan), cells were incubated for 1 h at 37 ℃. The cell viability was tested using a microplate reader at 450 nm (Molecular Devices, I3).

2.8 EdU assay

The 5-ethynyl-2'-deoxyuridine (EdU) assay was conducted to examine the cell proliferation using an EdU Detection kit (RiboBio, Guangzhou, China) following the manufacturer's protocols. Briefly, cells were incubated in DMEM containing 20 μmol/L EdU for 2 h. After fixing and permeabilization as described above, cells were stained with Apollo488 and Hoechst reagents in the dark. Images were taken by fluorescence microscopy (Olympus) and analyzed for EdU-positive cells by ImageJ.

2.9 Cell apoptosis assay

Cell apoptosis was tested using the Annexin V-FITC/propidium iodide (PI) Apoptosis Detection Kit (KeyGen, Nanjing, China). Cells were harvested and stained with 5 μL Annexin V-FITC and 5 μL PI for 15 min. Then, cell apoptosis was measured on a flow cytometer and analyzed by FlowJo 10.0 software (Tree-Star Inc., Ashland, OR, USA).

2.10 Wound healing assay

The wound healing assay was applied to evaluate cell migration. Cells were starved for 12 h before the confluent cell monolayer was scratched with a 100-μL pipette tip to create a wound. After washing with PBS, cells were cultured under different conditions with serum-free medium for 24 or 48 h, and imaged through a light microscope (CX22RFS1, Olympus, Tokyo, Japan). The wound area was calculated by ImageJ to assess the rate of cell migration.

2.11 Transwell matrigel assay

Cell invasion was determined by the transwell matrigel assay. Cells were seeded on the upper matrigel-coated transwell chamber in 24-well plates. They were then cultured with serum-free medium in the upper chamber, while DMEM containing 10% FBS was added to the lower chamber. After incubation for 48 h, the non-invading cells were gently wiped with a cotton swab, and invading cells were fixed with 4% paraformaldehyde and stained with 0.1% (1 g/L) crystal violet. The stained cells were visualized by a light microscope (CX22RFS1, Olympus) and counted by ImageJ.

2.12 Plasmids, siRNA, and transfection

The HIF-1α expression plasmid (pLenti-CMV-HIF-1α-3Flag), SERPINE1-promoter reporter plasmids, and respective empty plasmids were provided by OBiO Technology (Shanghai, China). For the luciferase assay, SERPINE1 promoter containing hypoxia-response element (HRE) was cloned into pGL4.10 vector to construct a wild-type reporter plasmid, and mutation at HRE motifs was introduced into the wild-type construct to generate a mutant reporter plasmid. The HIF-1α-luciferase reporter plasmid was purchased from YEASEN Biotechnology. All plasmids used in our study were confirmed by sequencing. The si-SERPINE1 and si-Control were obtained from GenePharma Technology (Shanghai, China). The small interfering RNA (siRNA) sequences are listed in Table S3. The applied siRNAs and plasmids were transfected into cells using Lipofectamine 3000 (Invitrogen, Carlsbad, CA, USA) according to the manufacturer's instructions.

2.13 Dual luciferase reporter assay

In 48-well plates, U87 and U251 cells were transfected with HIF-1α luciferase plasmid and Renilla plasmid (OBiO), and HEK293T cells were co-transfected with HIF-1α expression or empty plasmid and the indicated reporter plasmids of SERPINE1 together with Renilla control plasmid. After transfection for 24 h, cells were subjected to normoxia or hypoxia for additional 24 h, and then lysed to detect the luciferase activity using the dual-luciferase reporter assay system. The ratio of firefly signal to Renilla signal was used to assess the luciferase activity.

2.14 Bioinformatics analysis

The data of GBM patients were obtained from The Cancer Genome Atlas (TCGA; http://cancergenome.nih.gov). Gene Expression Profiling Interactive Analysis 2 (GEPIA2; http://gepia2.cancer-pku.cn/#index) was used to determine the expression levels of SERPINE1 in GBM and normal brain tissues. GEPIA2 was also used for survival analysis and correlation analysis of SERPINE1 in GBM patients. The Gene Set Enrichment Analysis (GSEA; http://www.gsea-msigdb.org/gsea/index.jsp) is often applied to determine whether a given set of genes displays statistical differences between two biological states (Subramanian et al., 2005). In this work, GSEA was performed to analyze possible pathways showing significant differences between high and low SERPINE1 groups using TCGA RNA sequencing (RNA-seq) datasets. The nominal *P*-value, false discovery rate (FDR) *q*-value, and normalized enrichment score (NES) were applied to denote the significance of associations between sets of genes and pathways (Li et al., 2021).

2.15 Statistical analysis

All values were expressed as mean±standard error of the mean (SEM) and analyzed by GraphPad Prism 8.0 software (San Diego, CA, USA). Statistical

analyses were performed by Student's *t*-test for comparison between two groups or one-way analysis of variance (ANOVA) for multiple comparisons. Two-way ANOVA was used for grouped comparisons. *P*-values of <0.05 were considered as statistical significance.

3 Results

3.1 Elevated ROS in hypoxic GBM cells

It has been reported that ROS are increased by hypoxia in various cancers (Chandel et al., 2000; Lei et al., 2014; Hu et al., 2017). Given that HIF-1α is rapidly increased in response to hypoxia (Weidemann and Johnson, 2008), the induction of hypoxia in GBM cells was confirmed by HIF-1α levels. As documented previously (Jin et al., 2018; Dabral et al., 2019), hypoxia promoted HIF-1α messenger RNA (mRNA) (Figs. 1a and S1a) and protein (Figs. 1b and S1b) expression, suggesting that the hypoxia models of GBM cells were successfully established. To determine the effects of hypoxia on ROS production in GBM cells, cellular ROS were measured using the DCFH-DA assay. The flow cytometry results showed that ROS levels were weak under normoxic conditions, but increased dramatically under hypoxic conditions, and were the highest at 12 h of hypoxia in U251 cells (Fig. 1c). To verify this result, ROS levels were further detected in U87 and LN229 cells using a fluorescence microscope for 2',7'-dichlorofluorescein (DCF) staining analysis. Consistently, more ROS were produced upon hypoxia than upon normoxia, and the highest levels of ROS were observed at 12 h after hypoxic exposure in U87 (Fig. 1d) and LN229 cells (Fig. S1c). However, ROS formation driven by hypoxia was significantly abolished by the ROS scavengers NAC (a non-specific ROS inhibitor) and DPI (an inhibitor of flavoproteins) in U87 and U251 cells (Fig. 1e). These results suggested that hypoxia led to ROS upregulation, which could be effectively inhibited by NAC and DPI in GBM cells.

3.2 Enhanced GBM progression by hypoxia-induced ROS

As second messengers, ROS are involved in a variety of cellular processes (Chiu and Dawes, 2012; Hurd et al., 2012), and play important roles in tumor progression (Lei et al., 2014; Chen et al., 2019; Sun et al., 2021). Our CCK-8 and EdU assays revealed that cell proliferation was notably increased in hypoxia, whereas scavenging ROS by NAC and DPI attenuated hypoxia-enhanced proliferation (Figs. 2a–2c). The effect of ROS on cell apoptosis was further determined by flow cytometry. Although hypoxia had no significant impact on GBM cell apoptosis compared with normoxia, cell apoptosis was elicited by NAC and DPI under hypoxic conditions (Fig. 2d). Moreover, hypoxia markedly potentiated the migration and invasion of U87 and U251 cells, and NAC and DPI reversed this phenomenon (Figs. 2e–2h). Accordingly, the expression of migration-associated genes was decreased by ROS inhibitors under hypoxia (Fig. S2). These data demonstrated that ROS were required for the hypoxia-enhanced proliferation, migration, and invasion in GBM cells.

3.3 Role of ROS in HIF-1α activation in hypoxic GBM cells

A large body of evidence proves that HIF-1α is a pivotal regulator of the adaptive responses to hypoxia (Semenza, 1998; Ke and Costa, 2006; Semenza, 2014), and ROS contribute to tumor progression through HIF-1α signaling (Xia et al., 2012; Zong et al., 2020; Sun et al., 2021). Hence, we hypothesized that ROS may regulate HIF-1α activation and then promote the adaptation to a low-oxygen environment in GBM cells. To investigate the role of ROS in HIF-1α activation, the cells were treated by hypoxia with or without ROS inhibitors (NAC or DPI). Indeed, hypoxia led to an increase in nuclear HIF-1α expression compared with normoxia (Fig. 3a). Conversely, the HIF-1α-inducing effect of hypoxia was nearly abrogated by NAC and DPI (Fig. 3a). Immunofluorescence results also indicated that more HIF-1α was accumulated in nuclei of U87 and U251 cells under hypoxia than under normoxia, whereas NAC and DPI attenuated hypoxia-elevated HIF-1α accumulation (Figs. 3b and S3). To further confirm the results above, we assessed HIF-1α transcriptional activity using a luciferase assay. Consistently, HIF-driven transcription was reinforced by hypoxia, which could be blocked by NAC and DPI (Fig. 3c). Collectively, these findings suggested that ROS mediated hypoxia-augmented HIF-1α expression in GBM cells.

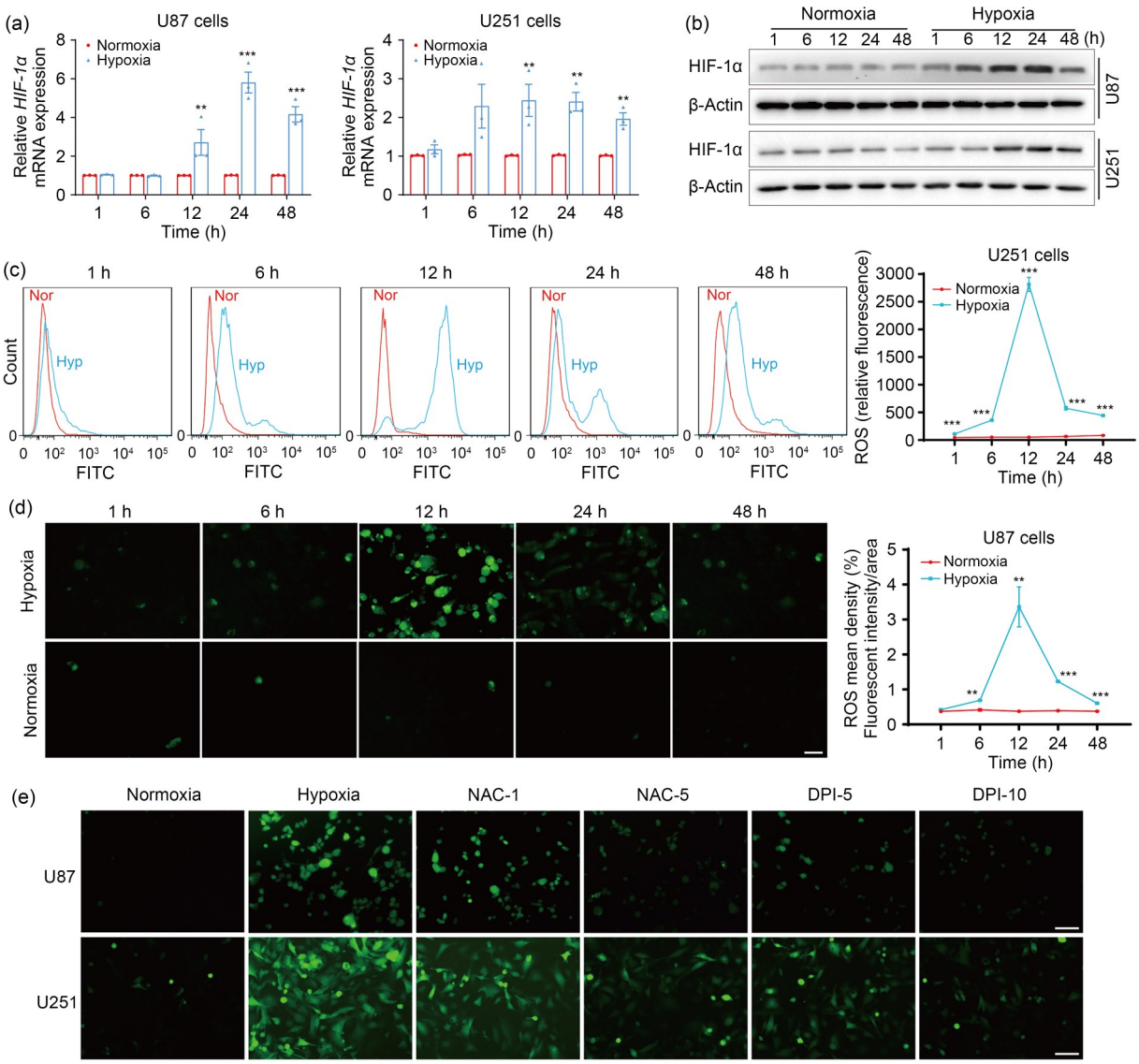

Fig. 1 Hypoxia increases intracellular ROS levels in GBM cells. (a, b) qPCR (a) and western blotting (b) were performed to detect the mRNA and protein expression, respectively, of HIF-1α at 1, 6, 12, 24, and 48 h after normoxic or hypoxic treatments. (c) Flow cytometry was used to assess ROS levels at the indicated time intervals after normoxic or hypoxic exposure. (d) ROS levels were determined using fluorescence under normoxia or hypoxia after the indicated time intervals (scale bar=100 μm). (e) ROS production was analyzed by fluorescence microscope when cells were pretreated with or without ROS inhibitors (NAC (1 or 5 mmol/L) or DPI (5 or 10 μmol/L)) for 4 h and then exposed to hypoxia for 12 h (scale bar=100 μm). The normoxia group was used as negative control. Data are expressed as mean±SEM (n=3). ** P<0.01, *** P<0.001, vs. normoxia group. ROS: reactive oxygen species; GBM: glioblastoma; qPCR: quantitative real-time polymerase chain reaction; mRNA: messenger RNA; HIF-1α: hypoxia-inducible factor-1α; NAC: *N*-acetyl-L-cysteine; DPI: diphenyleneiodonium chloride; SEM: standard error of the mean; Nor: normoxia; Hyp: hypoxia; FITC: fluorescein isothiocyanate.

3.4 Promoting effects of hypoxia-induced ROS on GBM migration and invasion via HIF-1α-dependent manner

Based on the findings that ROS stimulate HIF-1α activation under hypoxia, we conjectured that ROS may promote GBM progression via a HIF-1α-dependent manner under hypoxic conditions. To test this hypothesis, we overexpressed HIF-1α while scavenging ROS by NAC or DPI in U87 and U251 cells. As expected, HIF-1α overexpression abolished the reduced migration caused by ROS scavengers in part under hypoxic stress (Figs. 4a and 4b). Moreover, invasion inhibition by NAC or DPI was partially reversed by HIF-1α

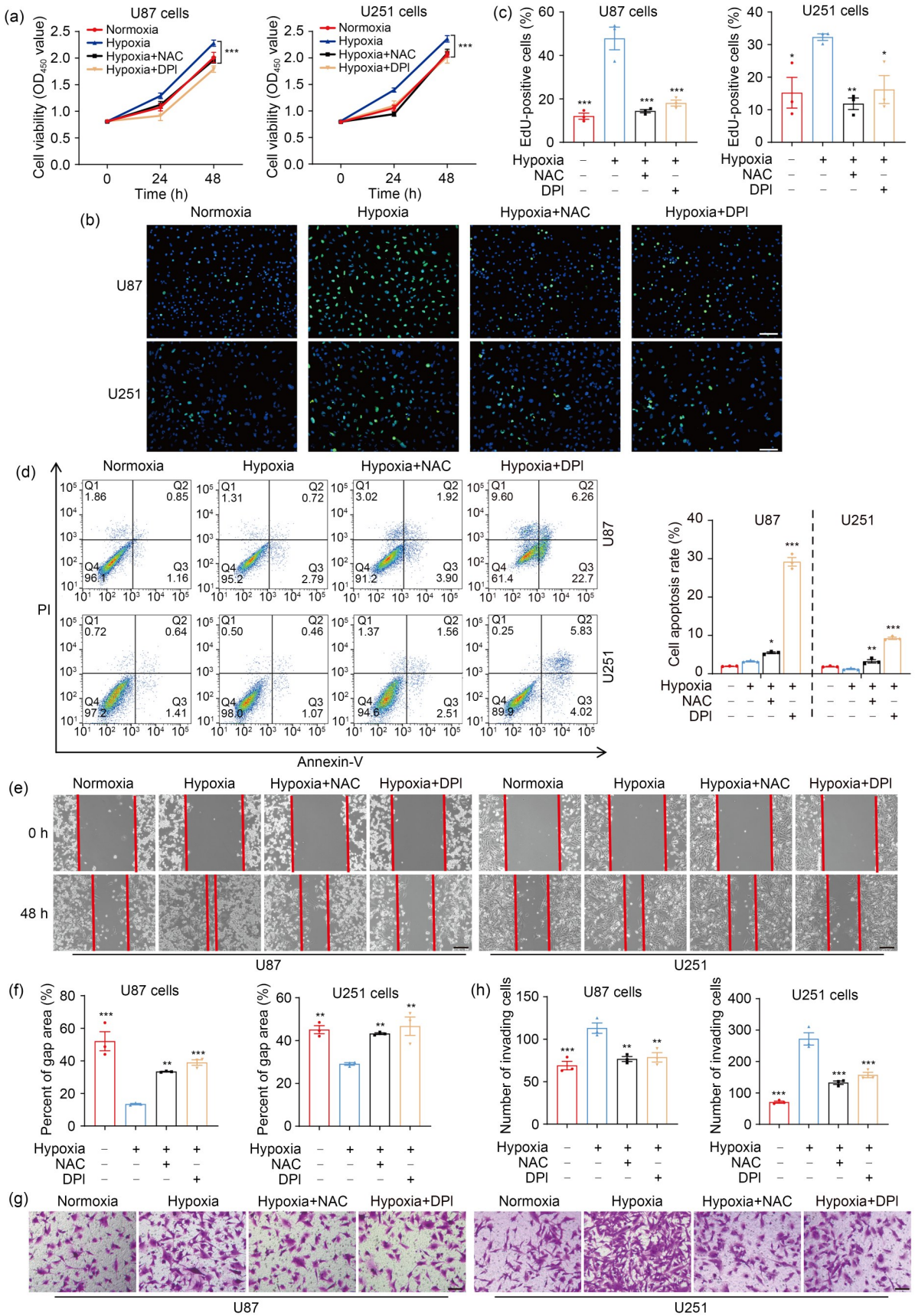
(a)
U87 cells
U251 cells
Normoxia
Hypoxia
Hypoxia+NAC
Hypoxia+DPI
Cell viability (OD450 value)
Time (h)
(b)
U87
U251
(c)
EdU-positive cells (%)
Hypoxia
NAC
DPI
(d)
PI
Annexin-V
Cell apoptosis rate (%)
(e)
0 h
48 h
(f)
Percent of gap area (%)
(g)
(h)
Number of invading cells

Fig. 2 ROS mediate hypoxia-promoted GBM progression. (a) CCK-8 assay was applied to examine the cell viability at 24 and 48 h. (b, c) EdU analysis was conducted to assess the cell proliferation ability at 48 h (scale bar=50 μm). (d) Flow cytometry was performed to detect the effect of ROS on cell apoptosis at 48 h. (e, f) The cell migration ability was measured by wound healing assay at 48 h (scale bar=200 μm). (g, h) The cell invasion ability was determined by transwell matrigel assay at 48 h (scale bar=100 μm). For all functional trials, the normoxia and hypoxia groups were used as negative and positive control, respectively, and the inhibitor groups were experimental groups. For experimental groups, cells were pretreated using NAC or DPI for 4 h before hypoxic exposure for the indicated time periods. Data are expressed as mean±SEM (n=3). * P<0.05, ** P<0.01, *** P <0.001, vs. hypoxia group. ROS: reactive oxygen species; GBM: glioblastoma; CCK-8: cell counting kit-8; EdU: 5-ethynyl-2'-deoxyuridine; NAC: *N*-acetyl-L-cysteine; DPI: diphenyleneiodonium chloride; SEM: standard error of the mean; OD_{450}: optical density value at 450 nm; PI: propidium iodide.

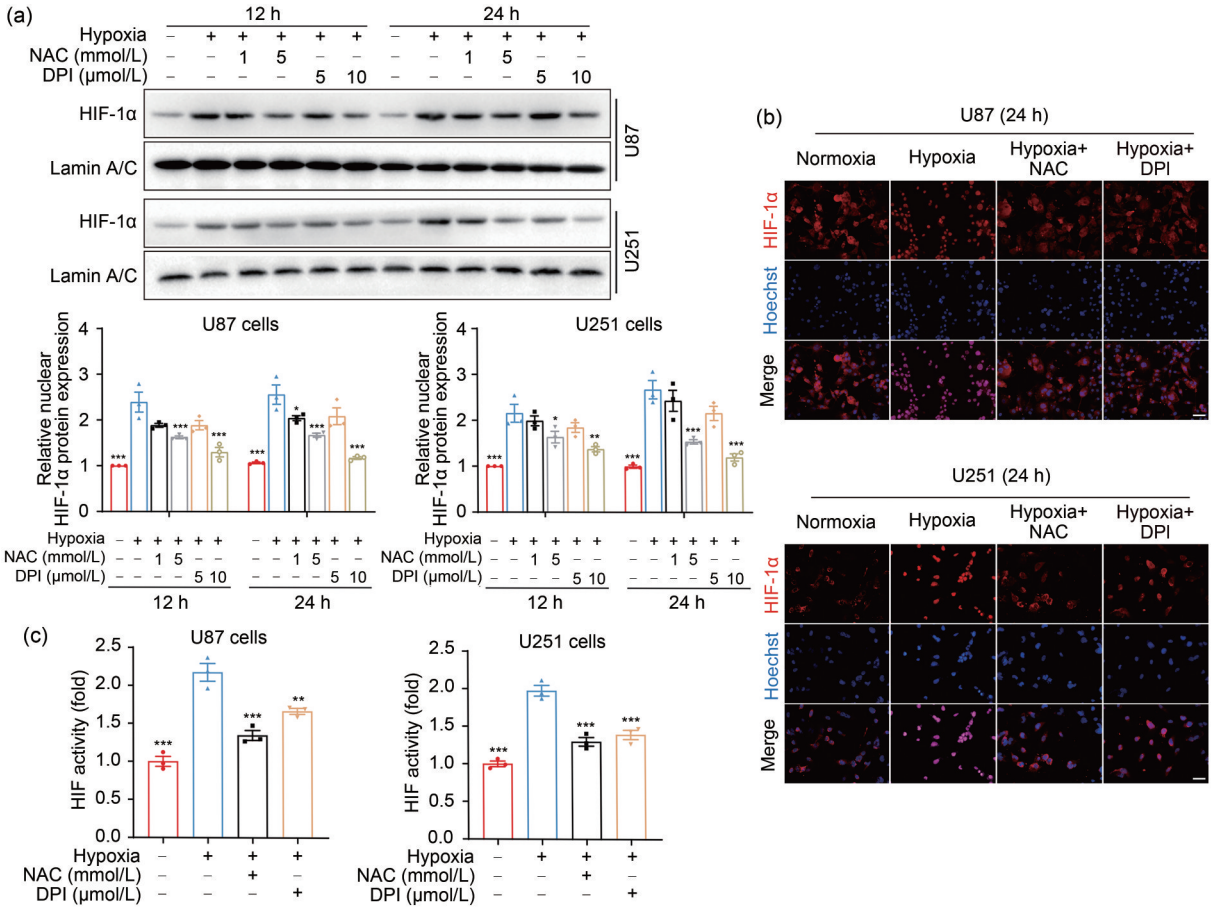

Fig. 3 Hypoxia-induced ROS drive HIF-1α activation in GBM cells. (a) The nuclear expression of HIF-1α protein was detected and quantified by western blotting after cells were incubated in the presence or absence of NAC (1 or 5 mmol/L) and DPI (5 or 10 μmol/L) for 4 h followed by hypoxia for 12 and 24 h. (b) The localization of HIF-1α was assessed by immunostaining in U87 and U251 cells under hypoxia 24 h after NAC (5 mmol/L) and DPI (10 μmol/L) treatment for 4 h (scale bar=25 μm). (c) Luciferase assay was performed to analyze the effect of ROS on HIF-1α activity. Cells that had been transfected using HIF-1α-luciferase plasmid for 20 h were treated with 5 mmol/L NAC or 10 μmol/L DPI for 4 h and then incubated under hypoxic conditions for 24 h. The normoxia group was used as negative control. Data are expressed as mean±SEM (n=3). * P<0.05, ** P<0.01, *** P<0.001, vs. hypoxia group. ROS: reactive oxygen species; HIF-1α: hypoxia-inducible factor-1α; GBM: glioblastoma; NAC: *N*-acetyl-L-cysteine; DPI: diphenyleneiodonium chloride; SEM: standard error of the mean.

overexpression under hypoxia exposure in U87 and U251 cells (Figs. 4c and 4d). Epithelial-mesenchymal transition (EMT) is known as a vital process in tumor invasion and metastasis (Polyak and Weinberg, 2009; Li et al., 2017; Sun et al., 2021). In the present study, DPI reduced the EMT-promoting effect of hypoxia, whereas this phenomenon was rescued by the over-expression of HIF-1α (Fig. 4e). These results indicated

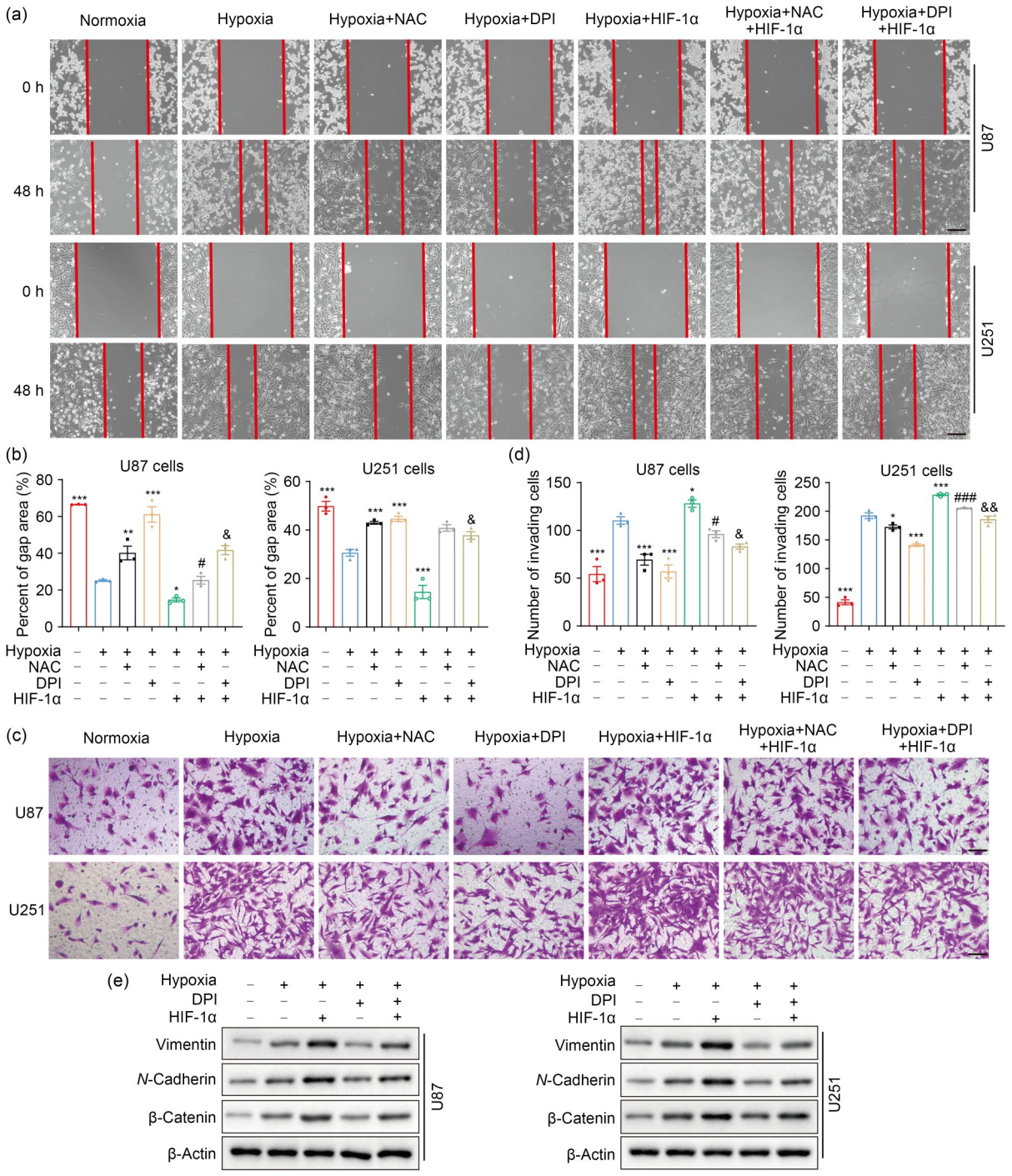

Fig. 4 ROS potentiate cell migration and invasion though HIF-1α signaling pathway in hypoxic GBM cells. (a, b) Scratch wound assay was used to test the effect of HIF-1α on cell migration under hypoxia for 48 h (scale bar=200 μm). (c, d) Matrigel invasion assay was performed to examine the effect of HIF-1α on cell invasion under hypoxia for 48 h (scale bar=100 μm). (e) The expression of EMT-related proteins under hypoxia for 24 h was detected by western blotting. For all experiments, cells were transfected with or without HIF-1α expression plasmid, and then incubated in the presence or absence of NAC or DPI for 4 h before hypoxia treatment for 24 or 48 h. The normoxia group was used as negative control. Data are expressed as mean±SEM (n=3). * P<0.05, ** P<0.01, *** P<0.001, vs. hypoxia group; $^{\#}$ P<0.05, $^{\#\#\#}$ P<0.001, vs. hypoxia+NAC group; $^{\&}$ P<0.05, $^{\&\&}$ P<0.01, vs. hypoxia+DPI group. ROS: reactive oxygen species; HIF-1α: hypoxia-inducible factor-1α; GBM: glioblastoma; EMT: epithelial-mesenchymal transition; NAC: *N*-acetyl-L-cysteine; DPI: diphenyleneiodonium chloride; SEM: standard error of the mean.

that the promoting effects of hypoxia-induced ROS on cell migration and invasion may depend on the HIF-1α pathway in GBM cells.

3.5 Upregulation of SERPINE1 transcription by HIF-1α

ROS, that can regulate gene expression (Kunsch and Medford, 1999), and HIF-1α, a central transcription factor upon hypoxia, are involved in the transcription of various target genes (Monteiro et al., 2017). Thus, we further explored the downstream mechanism by which ROS-HIF-1α axis promoted GBM EMT. Considering that the mesenchymal-related protein SERPINE1 is involved in GBM progression (Tang et al., 2021) and is elevated by hypoxia in GBM (Chédeville et al., 2020), the following work was performed to determine whether ROS-HIF-1α could regulate SERPINE1 expression under hypoxia. We first assessed the expression of SERPINE1 in GBM using public datasets. The results showed that SERPINE1 expression was higher in GBM tissues than in normal brain tissues (Fig. 5a). The survival analysis suggested that the median survival was significantly lower in GBM patients with high SERPINE1 expression than in those with low expression (Fig. 5b). The GSEA uncovered the significant ROS pathways and hypoxia enrichment in the higher SERPINE1 expression group (Fig. 5c). To confirm this result, U87 and U251 cells were exposed to hypoxia for the indicated time periods, and subjected to the detection of SERPINE1 expression and secretion. Indeed, hypoxia exposure strongly upregulated SERPINE1 mRNA (Fig. 5d) and protein expression (Fig. 5e). A marked increase in SERPINE1 secretion was also observed under hypoxia (Fig. 5f). Furthermore, we investigated the regulation effects of HIF-1α and ROS on SERPINE1 expression. HIF-1α overexpression and ROS deprivation with DPI respectively upregulated and downregulated SERPINE1 in hypoxia, and the decreased SERPINE1 expression caused by DPI was rescued by the overexpression of HIF-1α (Figs. 5g–5i). Previous research has reported that HIF-1α, as a transcription factor of SERPINE1, positively regulated its transcription (Fink et al., 2002). Bioinformatics analyses revealed that HIF-1α expression was positively correlated with SERPINE1 in GBM (Fig. 5j). Therefore, we further clarified whether HIF-1α transcriptionally regulated SERPINE1. Based on the fact that the conserved sequences of HRE are 5'-RCGTG-3', JASPAR analysis found the putative HIF-binding sites (HBSs) at the *SERPINE1* promoter (Fig. 5k). Given that HRE-2 (5'-cacgtaca-3'; our predicted sequence: 5'-acacgtacac-3') was reported to be the site where HIF-1α binds to *SERPINE1* promoter (Fink et al., 2002), we constructed SERPINE1 wild-type and HRE-2-mutant reporter plasmids. In the luciferase assay, the luciferase activity of SERPINE1 was profoundly increased when HIF-1α was overexpressed, which could be blocked by the deletion of HRE2 in the SERPINE1 promoter (Fig. 5l). To summarize, the above evidence proved that hypoxia-induced SERPINE1 is mediated by HIF-1α binding to the *SERPINE1* promoter.

3.6 Role of ROS-HIF-1α-SERPINE1 in GBM progression under hypoxia

In order to determine the involvement of SERPINE1 in the adaptation of GBM cells to hypoxia, we knocked down SERPINE1 in U87 and U251 cells (Figs. 6a, 6b, and S4a). SERPINE1 deficiency significantly inhibited cell migration under hypoxia (Figs. S4b and S4c). Consistently, SERPINE1 knockdown restricted the invasion ability of U87 and U251 cells under hypoxic conditions (Figs. S4d and S4e). These data suggested that SERPINE1 may be involved in the invasion and migration led by hypoxia. To further reveal the role of the HIF-1α-SERPINE1 axis, HIF-1α was overexpressed while SERPINE1 was knocked down (Fig. 6c). The results showed that SERPINE1 knockdown reversed enhanced cell migration and invasion resulting from HIF-1α overexpression under hypoxia (Figs. 6d–6f). In addition, GSEA analysis on TCGA datasets revealed a significant EMT enrichment in the SERPINE1 expression group (Fig. 6g). We next investigated whether SERPINE1 mediated the EMT process promoted by HIF-1α under hypoxia. The results showed that the excessive expression of HIF-1α decreased the epithelial marker E-cadherin, and increased the mesenchymal markers *N*-cadherin, vimentin, and β-catenin, but SERPINE1 deficiency reversed this phenomenon (Fig. 6h). These findings indicated that the HIF-1α-SERPINE1 pathway played a role in GBM progression under an oxygen-deficient milieu.

4 Discussion

In this work, we identified a feasible mechanism by which hypoxia promotes GBM migration

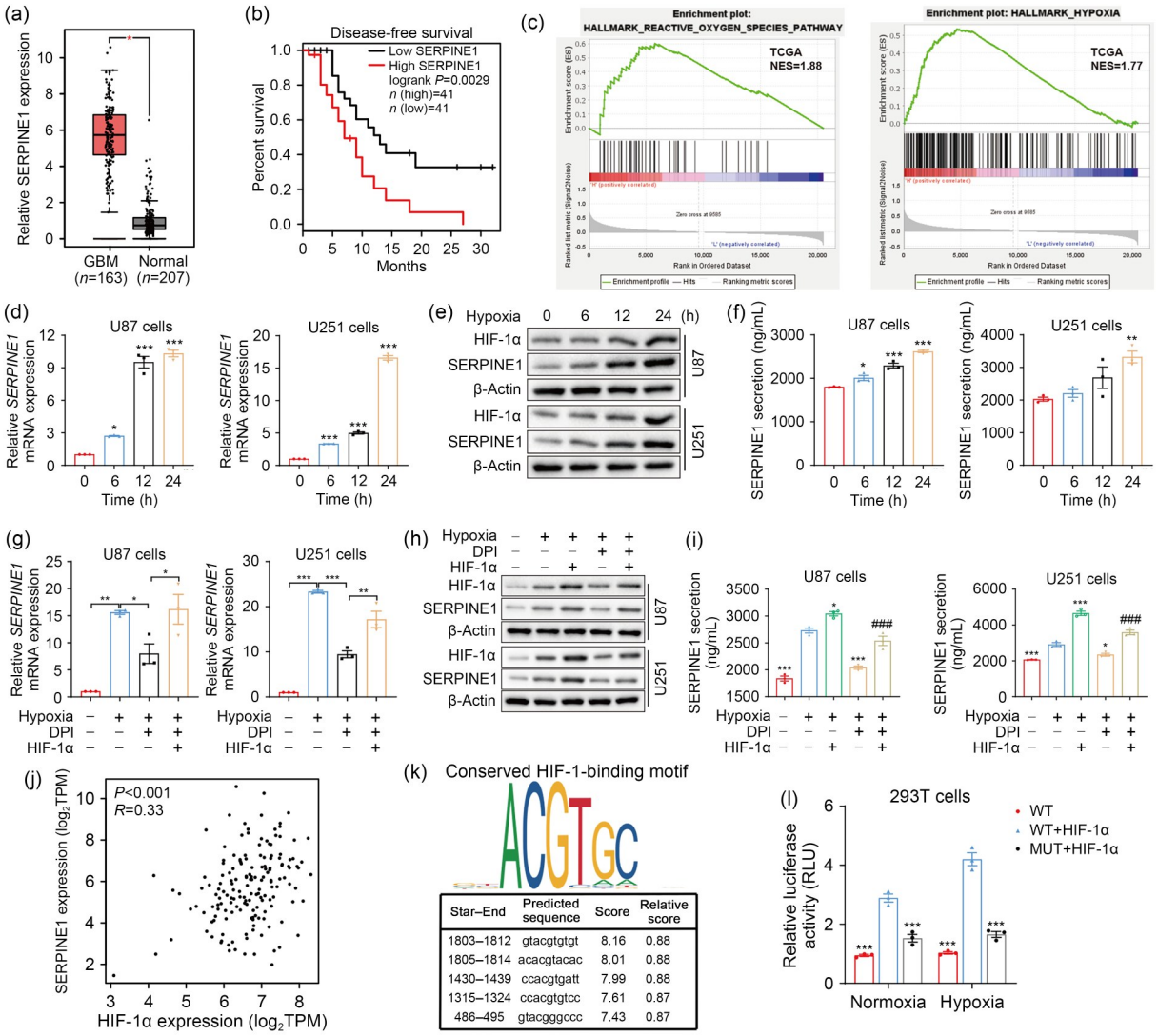

Fig. 5 ***SERPINE1*** **is the downstream gene of the ROS-HIF-1α axis. (a) SERPINE1 expression in GBM and normal tissues was analyzed on the TCGA datasets using GEPIA2. (b) The GEPIA2 website was used for the survival analysis (cutoff: median) of GBM patients in terms of high SERPINE1 expression vs. low SERPINE1 expression. (c) GSEA analysis was conducted to determine ROS pathway and hypoxia enrichment in SERPINE1-high GBM tissues. (d, e) The mRNA (d) and protein (e) expression levels of SERPINE1 were detected at 6, 12, and 24 h under normoxic or hypoxic environment. (f) The levels of extracellular SERPINE1 were examined by ELISA kits at the indicated normoxia or hypoxia intervals. * *P*<0.05, ** *P*<0.01, *** *P*<0.001, vs. 0 h group. (g–i) qPCR (g), western blotting (h), and ELISA (i) analyses were performed to assess the effects of ROS and HIF-1α on SERPINE1 expression and secretion. Cells were transfected with or without HIF-1α expression plasmid for 20 h, and then treated using 10 μmol/L DPI followed by hypoxic stimulus for 24 h. * *P*<0.05, ** *P*<0.01, *** *P*<0.001, vs. hypoxia group; ### *P*<0.001, vs. hypoxia+HIF-1α group. (j) SERPINE1 expression was plotted as a function of HIF-1α expression using GEPIA2 (correlation coefficient: Spearman). (k) JASPAR analysis was performed to find the possible sites where HIF-1α binds to** ***SERPINE1*** **promoters. (l) Luciferase assay was conducted to analyze the effect of HIF-1α on SERPINE1 activity under normoxia and hypoxia. For normoxic treatments, cells were transfected with SERPINE1 reporter plasmids (WT or MUT) and/or HIF-1α expression plasmid for 48 h. For hypoxic treatments, cells were transfected with the above plasmids under normoxia for 24 h and then under hypoxia for another 24 h. *** *P*<0.001, vs. WT+HIF-1α group. Data are expressed as mean±SEM (*n*=3). SERPINE1: serine protease inhibitor family E member 1; ROS: reactive oxygen species; HIF-1α: hypoxia-inducible factor-1α; GBM: glioblastoma; TCGA: The Cancer Genome Atlas; GEPIA2: Gene Expression Profiling Interactive Analysis 2; GSEA: Gene Set Enrichment Analysis; mRNA: messenger RNA; ELISA: enzyme-linked immunosorbent assay; qPCR: quantitative real-time polymerase chain reaction; DPI: diphenyleneiodonium chloride; WT: wild-type; MUT: mutant type; SEM: standard error of the mean; NES: normalized enrichment score; TPM: transcripts per million; RLU: relative luciferase unit.**

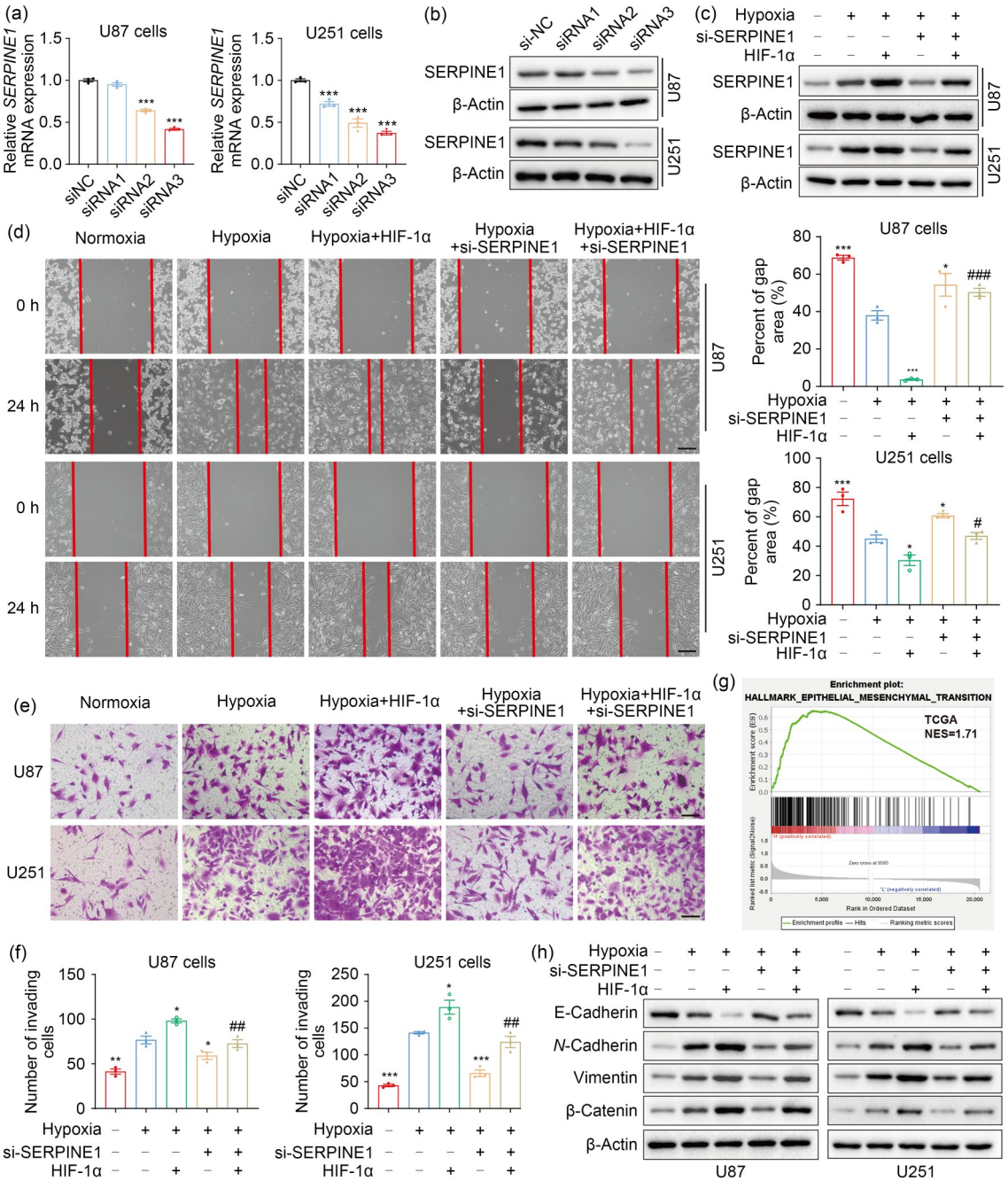

Fig. 6 ROS enhance GBM adaptation to hypoxia via the HIF-1α-SERPINE1 pathway. (a, b) qPCR (a) and western blotting (b) were conducted to examine the efficiency of SERPINE1 knockdown in U87 and U251 cells. * *P*<0.001, vs. siNC group. (c) The expression levels of SERPINE1 were measured in U87 and U251 cells, where SERPINE1 was knocked down or/and HIF-1α was overexpressed. (d) The role of SERPINE1 in cell migration was assessed by wound healing assay under hypoxia for 24 h (scale bar=200 μm). (e, f) The role of SERPINE1 in cell invasion was detected by matrigel invasion assay under hypoxia for 24 h (scale bar=100 μm). * *P*<0.05, ** *P*<0.01, *** *P*<0.001, vs. hypoxia group; # *P*<0.05, ## *P*<0.01, ### *P*<0.001, vs. hypoxia+HIF-1α group. (g) GSEA analysis was performed to determine EMT enrichment in SERPINE1-high GBM tissues. (h) Western blotting was used to examine the levels of EMT-related proteins under hypoxia for 24 h. Cells were transfected with siRNA targeting SERPINE1 or/and plasmid expressing HIF-1α for 24 h, and then subjected to hypoxia for 24 h. The normoxia group was used as negative control. Data are expressed as mean±SEM (*n*=3). ROS: reactive oxygen species; GBM: glioblastoma; HIF-1α: hypoxia-inducible factor-1α; SERPINE1: serine protease inhibitor family E member 1; qPCR: quantitative real-time polymerase chain reaction; NC: negative control; GSEA: Gene Set Enrichment Analysis; EMT: epithelial-mesenchymal transition; siRNA: small interfering RNA; si: siRNA; SEM: standard error of the mean; mRNA: messenger RNA; TCGA: The Cancer Genome Atlas; NES: normalized enrichment score.**

and invasion, and unraveled the essential role of the ROS-HIF-1α-SERPINE1 axis in the hypoxic adaptation of GBM cells (Fig. 7). Elevated ROS levels were observed under a hypoxic microenvironment. It was also revealed that ROS attenuation using ROS scavengers inhibits the proliferation, migration, and invasion of GBM cells and facilitates their apoptosis during hypoxia. Furthermore, we investigated how hypoxia-stimulated ROS help GBM adapt to hypoxic conditions: hypoxia-induced ROS activate HIF-1α signaling, and in turn HIF-1α drives the hypoxic induction of SERPINE1 via direct transcriptional regulation, which assists GBM cells with coping with hypoxic stress.

Hypoxia is a crucial characteristic of GBM microenvironments (Dao Trong et al., 2018), and is involved in an array of malignant behaviors including tumor proliferation, invasion, and EMT (Jin et al., 2018; Srivastava et al., 2018; Zhang et al., 2018). Our functional experiments demonstrated that hypoxia strongly promotes GBM cell proliferation, migration, and invasion. Hypoxia has been reported to enhance cell proliferation in various tumors, including non-small cell lung cancer (Chen et al., 2020), lung adenocarcinoma (Zhang et al., 2021), hepatocellular carcinoma (Carreres et al., 2022), and uterine leiomyoma (Miyashita-Ishiwata et al., 2022). Under hypoxic microenvironments, multiple signaling pathways are stimulated, with ROS delivery being one of the key determinants of tumor adaptation to hypoxia. It has been documented that ROS have higher level in a large number of tumor cells than normal cells, but they exhibit a "two-sided" effect: increased ROS contribute to tumor growth as "good" molecules, while excessive ROS restrict tumor growth as "bad" molecules (Chandel et al., 2000; Watson, 2013; Ge et al., 2017). Therefore, maintaining ROS homeostasis is of vital importance for preventing tumor cells from causing oxidative stress damages.

Consistent with previous reports (Yang Y et al., 2020; Wu et al., 2021), the present study showed that ROS accumulation is induced by hypoxic stimuli. It is known that nicotinamide adenine dinucleotide phosphate (NADPH) oxidase (NOX, e.g., NOX1 and NOX4) is a key enzyme for redox signaling and the major source of ROS (Spencer and Engelhardt, 2014). After hypoxic exposure, NOX4 was increased and was a major contributor to upregulated ROS levels in pulmonary arterial smooth muscle cells (PASMCs) (Mittal et al., 2012). Another study suggested that siRNA targeting NOX1 reduces acute hypoxia-induced increase in the Ras association domain family 1 isoform A (RASSF1A) protein in PASMC via inhibiting ROS formation (Dabral et al., 2019). In addition, under hypoxic conditions, the oxidation of nicotinamide adenine dinucleotide (NAD)-related substrate (complex I) was changed to the oxidation of succinate (complex II) (Lukyanova et al., 2018). ROS are produced by complex II when the activity of other complexes (complex I/III) is inhibited (Quinlan et al., 2012; Dröse, 2013). Interestingly, our work indicated that ROS levels were reduced with prolonged exposure to hypoxia, but were still higher than those under normoxic conditions,

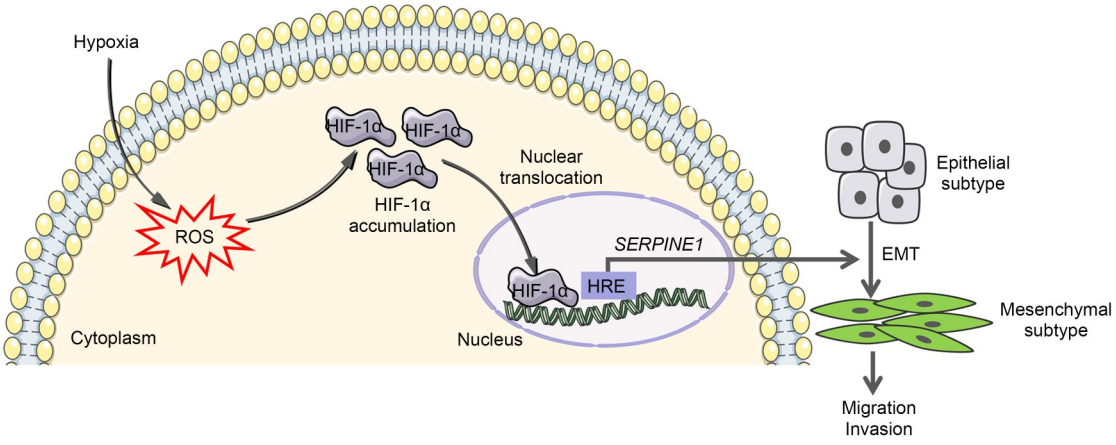

Fig. 7 Summary of our result findings in this study. Hypoxia promotes the generation of ROS in GBM cells, and elevated ROS contribute to HIF-1α accumulation and nuclear translocation. HIF-1α upregulates SERPINE1 by binding to the HRE of *SERPINE1* promoter, thereby promoting GBM migration and invasion through EMT. ROS may be potential therapeutic targets of GBM. ROS: reactive oxygen species; GBM: glioblastoma; HIF-1α: hypoxia-inducible factor-1α; SERPINE1: serine protease inhibitor family E member 1; HRE: hypoxia response element; EMT: epithelial-mesenchymal transition.

indicating that ROS levels may be extremely high under hypoxic conditions. Further investigations revealed that hypoxia-triggered pro-tumor effects were diminished when sweeping ROS, suggesting that ROS levels elicited by hypoxia are moderate in GBM cells and ROS function as "good" molecules to help them adapt to low-oxygen environments (Zong et al., 2020). However, the exact mechanism of removing excessive ROS and maintaining ROS balance under hypoxia remains a poorly studied field.

It is well-known that HIF-1α is a central regulator of hypoxic adaptation. Herein, a dramatic increase in HIF-1α was observed in response to hypoxic stress. Of note, the trends of HIF-1α expression and ROS generation are similar upon hypoxia, that is, their levels elevate and then reduce with prolonged hypoxia, indicating the regulatory role of ROS in HIF-1α activation. However, paradoxical data documented that ROS activate epidermal growth factor receptor (EGFR) signaling but not the HIF-1α pathway in MDA-MB-468 breast cancer cells under an O_2-deficient milieu (Azimi et al., 2017). Another study also implied that HIF-1α stability in hypoxia is independent of mitochondrial ROS (Chua et al., 2010). Inversely, increasing lines of evidence point to the possibility that ROS produced by mitochondrial complex III are required for hypoxia-driven HIF-1α activation (Chandel et al., 1998; Klimova and Chandel, 2008; Ivan and Kaelin, 2017), and stabilize HIF-1α via regulating prolyl hydroxylase (PHD) (Schumacker, 2011; Niecknig et al., 2012; Schieber and Chandel, 2014). In this work, we showed that endogenous ROS mediate HIF-1α induction led by hypoxia, which potentiates GBM progression through promoting EMT under hypoxic conditions.

EMT, a shift from the epithelial to the mesenchymal state, is an important process to accelerate tumor motility in hypoxia (Thiery et al., 2009; Tsai and Yang, 2013; Peng et al., 2020; Chen et al., 2021). EMT is an important biological process in which epithelial cells lose cell polarity and cell-cell contacts, and obtain a highly motile and invasive mesenchymal phenotype (Zheng and Kang, 2014). Various factors are involved in the EMT process, some of them increasing (*N*-cadherin, vimentin, Snail, zinc finger E-box binding homeobox 1 (ZEB1), and Twist) and E-cadherin decreasing. It was documented that Snail, Twist, ZEB1, and other EMT regulators mediate hypoxia-induced EMT (Lu and Kang, 2019; Yang J et al., 2020). Our work confirmed that Snail and Twist, but not ZEB1, are upregulated (Fig. S2) and EMT-related proteins are also induced when cells are exposed to hypoxia. Accumulating studies have illustrated that SERPINE1 facilitates cell EMT, migration, and invasion (Wang et al., 2019; Li X et al., 2020), and is even thought to be a biomarker related to EMT in gastric cancer (Xu et al., 2019). In breast cancer, SERPINE1 promotes tumor metastasis through enhancing the EMT process (Li SJ et al., 2020). A variety of non-coding RNAs regulate EMT via targeting SERPINE1 (Li X et al., 2020; Yang et al., 2021; Liu et al., 2022). EMT plays an important role in cancer metastasis and invasion (Hou et al., 2014; Li et al., 2017). However, whether SERPINE1 enhances EMT in hypoxic GBM cells is unclear. Herein, we elucidated that ROS drive the hypoxic induction of SERPINE1 via the transcriptional regulation of HIF-1α. Functionally, SERPINE1 mediates the HIF-1α-promoted migration, invasion, and EMT of GBM cells during low-O_2 environments. A growing number of researches have clarified that SERPINE1 promotes glucose metabolism in breast cancer (Humphries et al., 2019; Xu et al., 2021). However, the role of SERPINE1 in GBM glycolytic metabolism has not been explored, which is being investigated by our group (unpublished).

5 Conclusions

We demonstrated that the ROS-HIF-1α-SERPINE1 pathway favors GBM progression under hypoxic conditions. This study deepens our understanding of GBM adaptation to hypoxia, and provides new evidence for ROS as therapeutic targets of GBM.

Acknowledgments

We thank the supports from Hasenbio Technology Company (Wuxi, China) and the Public Experimental Research Center of Xuzhou Medical University (Xuzhou, China). This study was supported by the National Natural Science Foundation of China (Nos. 81772688 and 81372698), the Priority Academic Program Development of Jiangsu Higher Education Institutions (PAPD), the Research Foundation for Talented Scholars of Xuzhou Medical University (No. RC20552223), and the Postgraduate Research & Practice Innovation Program of Jiangsu Province (No. KYCX20_2463), China.

Author contributions

Lin ZHANG and Yuanyuan CAO conceived and designed the study, performed the experiments and data analysis, and wrote and edited the manuscript. Xiaoxiao GUO and Xiaoyu WANG performed the experiments, analyzed the data, and drafted the manuscript. Xiao HAN performed data analysis and figure arrangements. Kouminin KANWORE checked the data and drafted the manuscript. Xiaoliang HONG and Han ZHOU provided technical supports. Dianshuai GAO supervised and conceived this work, and wrote the manuscript. All authors have reviewed and approved the final manuscript, and therefore, have full access to all the data in the work and take responsibility for the integrity and security of the data.

Compliance with ethics guidelines

Lin ZHANG, Yuanyuan CAO, Xiaoxiao GUO, Xiaoyu WANG, Xiao HAN, Kouminin Kanwore, Xiaoliang HONG, Han ZHOU, and Dianshuai GAO declare that they have no conflict of interest.

This article does not contain any studies with human or animal subjects performed by any of the authors.

References

Andrew AS, Klei LR, Barchowsky A, 2001. Nickel requires hypoxia-inducible factor-1α, not redox signaling, to induce plasminogen activator inhibitor-1. *Am J Physiol Lung Cell Mol Physiol*, 281(3):L607-L615. https://doi.org/10.1152/ajplung.2001.281.3.L607

Azimi I, Petersen RM, Thompson EW, et al., 2017. Hypoxia-induced reactive oxygen species mediate N-cadherin and SERPINE1 expression, EGFR signalling and motility in MDA-MB-468 breast cancer cells. *Sci Rep*, 7:15140. https://doi.org/10.1038/s41598-017-15474-7

Carreres L, Mercey-Ressejac M, Kurma K, et al., 2022. Chronic intermittent hypoxia increases cell proliferation in hepatocellular carcinoma. *Cells*, 11(13):2051. https://doi.org/10.3390/cells11132051

Chandel NS, Maltepe E, Goldwasser E, et al., 1998. Mitochondrial reactive oxygen species trigger hypoxia-induced transcription. *Proc Natl Acad Sci USA*, 95(20):11715-11720. https://doi.org/10.1073/pnas.95.20.11715

Chandel NS, McClintock DS, Feliciano CE, et al., 2000. Reactive oxygen species generated at mitochondrial complex III stabilize hypoxia-inducible factor-1α during hypoxia: a mechanism of O_2 sensing. *J Biol Chem*, 275(33):25130-25138. https://doi.org/10.1074/jbc.M001914200

Chédeville AL, Lourdusamy A, Monteiro AR, et al., 2020. Investigating glioblastoma response to hypoxia. *Biomedicines*, 8(9):310. https://doi.org/10.3390/biomedicines8090310

Chen CL, Wang SC, Liu P, 2019. Deferoxamine enhanced mitochondrial iron accumulation and promoted cell migration in triple-negative MDA-MB-231 breast cancer cells via a ROS-dependent mechanism. *Int J Mol Sci*, 20(19):4852. https://doi.org/10.3390/ijms20194952

Chen D, Wu YX, Qiu YB, et al., 2020. Hyperoside suppresses hypoxia-induced A549 survival and proliferation through ferrous accumulation via AMPK/HO-1 axis. *Phytomedicine*, 67:153138. https://doi.org/10.1016/j.phymed.2019.153138

Chen XT, Li ZW, Yong HM, et al., 2021. Trim21-mediated HIF-1α degradation attenuates aerobic glycolysis to inhibit renal cancer tumorigenesis and metastasis. *Cancer Lett*, 508:115-126. https://doi.org/10.1016/j.canlet.2021.03.023

Chiu J, Dawes IW, 2012. Redox control of cell proliferation. *Trends Cell Biol*, 22(11):592-601. https://doi.org/10.1016/j.tcb.2012.08.002

Chua YL, Dufour E, Dassa EP, et al., 2010. Stabilization of hypoxia-inducible factor-1α protein in hypoxia occurs independently of mitochondrial reactive oxygen species production. *J Biol Chem*, 285(41):31277-31284. https://doi.org/10.1074/jbc.M110.158485

Dabral S, Muecke C, Valasarajan C, et al., 2019. A RASSF1A-HIF1α loop drives Warburg effect in cancer and pulmonary hypertension. *Nat Commun*, 10:2130. https://doi.org/10.1038/s41467-019-10044-z

Dao Trong P, Rösch S, Mairbäurl H, et al., 2018. Identification of a prognostic hypoxia-associated gene set in IDH-mutant glioma. *Int J Mol Sci*, 19(10):2903. https://doi.org/10.3390/ijms19102903

Dröse S, 2013. Differential effects of complex II on mitochondrial ROS production and their relation to cardioprotective pre- and postconditioning. *Biochim Biophys Acta Bioenerget*, 1827(5):578-587. https://doi.org/10.1016/j.bbabio.2013.01.004

Fandrey J, Gassmann M, 2009. Oxygen sensing and the activation of the hypoxia inducible factor 1 (HIF-1)–*Invited Article*. *In*: Gonzalez C, Nurse CA, Peers C (Eds.), Arterial Chemoreceptors. Advances in Experimental Medicine and Biology, Vol. 648. Springer, Dordrecht, p.197-206. https://doi.org/10.1007/978-90-481-2259-2_23

Fink T, Kazlauskas A, Poellinger L, et al., 2002. Identification of a tightly regulated hypoxia-response element in the promoter of human plasminogen activator inhibitor-1. *Blood*, 99(6):2077-2083. https://doi.org/10.1182/blood.v99.6.2077

Ge WJ, Zhao KM, Wang XW, et al., 2017. iASPP is an antioxidative factor and drives cancer growth and drug resistance by competing with Nrf2 for Keap1 binding. *Cancer Cell*, 32(5):561-573.6. https://doi.org/10.1016/j.ccell.2017.09.008

Harris AL, 2002. Hypoxia—a key regulatory factor in tumour growth. *Nat Rev Cancer*, 2(1):38-47. https://doi.org/10.1038/nrc704

Hou P, Zhao Y, Li Z, et al., 2014. LincRNA-ROR induces epithelial-to-mesenchymal transition and contributes to breast cancer tumorigenesis and metastasis. *Cell Death Dis*, 5(6):e1287. https://doi.org/10.1038/cddis.2014.249

Hu ZZ, Dong N, Lu D, et al., 2017. A positive feedback loop between ROS and Mxi1-0 promotes hypoxia-induced VEGF expression in human hepatocellular carcinoma

cells. *Cell Signal*, 31:79-86.
https://doi.org/10.1016/j.cellsig.2017.01.007

Humphries BA, Buschhaus JM, Chen YC, et al., 2019. Plasminogen activator inhibitor 1 (PAI1) promotes actin cytoskeleton reorganization and glycolytic metabolism in triple-negative breast cancer. *Mol Cancer Res*, 17(5):1142-1154.
https://doi.org/10.1158/1541-7786.MCR-18-0836

Hurd TR, DeGennaro M, Lehmann R, 2012. Redox regulation of cell migration and adhesion. *Trends Cell Biol*, 22(2):107-115.
https://doi.org/10.1016/j.tcb.2011.11.002

Ivan M, Kaelin WG, 2017. The EGLN-HIF O_2-sensing system: multiple inputs and feedbacks. *Mol Cell*, 66(6):772-779.
https://doi.org/10.1016/j.molcel.2017.06.002

Jin P, Shin SH, Chun YS, et al., 2018. Astrocyte-derived CCL20 reinforces HIF-1-mediated hypoxic responses in glioblastoma by stimulating the CCR6-NF-κB signaling pathway. *Oncogene*, 37(23):3070-3087.
https://doi.org/10.1038/s41388-018-0182-7

Ke QD, Costa M, 2006. Hypoxia-inducible factor-1 (HIF-1). *Mol Pharmacol*, 70(5):1469-1480.
https://doi.org/10.1124/mol.106.027029

Kessler J, Hahnel A, Wichmann H, et al., 2010. HIF-1α inhibition by siRNA or chetomin in human malignant glioma cells: effects on hypoxic radioresistance and monitoring via CA9 expression. *BMC Cancer*, 10:605.
https://doi.org/10.1186/1471-2407-10-605

Klimova T, Chandel NS, 2008. Mitochondrial complex III regulates hypoxic activation of HIF. *Cell Death Differ*, 15(4):660-666.
https://doi.org/10.1038/sj.cdd.4402307

Kunsch C, Medford RM, 1999. Oxidative stress as a regulator of gene expression in the vasculature. *Circ Res*, 85(8):753-766.
https://doi.org/10.1161/01.res.85.8.753

Lei JJ, Huo XW, Duan WX, et al., 2014. α-Mangostin inhibits hypoxia-driven ROS-induced PSC activation and pancreatic cancer cell invasion. *Cancer Lett*, 347(1):129-138.
https://doi.org/10.1016/j.canlet.2014.02.003

Li SJ, Wei XH, Zhan XM, et al., 2020. Adipocyte-derived leptin promotes PAI-1-mediated breast cancer metastasis in a STAT3/miR-34a dependent manner. *Cancers (Basel)*, 12(12):3864.
https://doi.org/10.3390/cancers12123864

Li X, Wu P, Tang YY, et al., 2020. Down-regulation of *miR-181c-5p* promotes epithelial-to-mesenchymal transition in laryngeal squamous cell carcinoma *via* targeting *SERPINE1*. *Front Oncol*, 10:544476.
https://doi.org/10.3389/fonc.2020.544476

Li X, Zuo HW, Zhang L, et al., 2021. Validating *HMMR* expression and its prognostic significance in lung adenocarcinoma based on data mining and bioinformatics methods. *Front Oncol*, 11:720302.
https://doi.org/10.3389/fonc.2021.720302

Li XD, Dong P, Wei WS, et al., 2019. Overexpression of CEP72 promotes bladder urothelial carcinoma cell aggressiveness via epigenetic CREB-mediated induction of SERPINE1. *Am J Pathol*, 189(6):1284-1297.
https://doi.org/10.1016/j.ajpath.2019.02.014

Li ZW, Hou PF, Fan DM, et al., 2017. The degradation of EZH2 mediated by lncRNA ANCR attenuated the invasion and metastasis of breast cancer. *Cell Death Differ*, 24(1):59-71.
https://doi.org/10.1038/cdd.2016.95

Liu L, Xiao S, Wang Y, et al., 2022. Identification of a novel circular RNA circZNF652/miR-486-5p/SERPINE1 signaling cascade that regulates cancer aggressiveness in glioblastoma (GBM). *Bioengineered*, 13(1):1411-1423.
https://doi.org/10.1080/21655979.2021.2018096

Lu W, Kang YB, 2019. Epithelial-mesenchymal plasticity in cancer progression and metastasis. *Dev Cell*, 49(3):361-374.
https://doi.org/10.1016/j.devcel.2019.04.010

Lukyanova LD, Kirova YI, Germanova EL, 2018. The role of succinate in regulation of immediate HIF-1α expression in hypoxia. *Bull Exp Biol Med*, 164(3):298-303.
https://doi.org/10.1007/s10517-018-3976-2

Mittal M, Gu XQ, Pak O, et al., 2012. Hypoxia induces K_v channel current inhibition by increased NADPH oxidase-derived reactive oxygen species. *Free Radic Biol Med*, 52(6):1033-1042.
https://doi.org/10.1016/j.freeradbiomed.2011.12.004

Miyashita-Ishiwata M, el Sabeh M, Reschke LD, et al., 2022. Hypoxia induces proliferation via NOX4-mediated oxidative stress and TGF-β3 signaling in uterine leiomyoma cells. *Free Radic Res*, 56(2):163-172.
https://doi.org/10.1080/10715762.2022.2061967

Monteiro AR, Hill R, Pilkington GJ, et al., 2017. The role of hypoxia in glioblastoma invasion. *Cells*, 6(4):45.
https://doi.org/10.3390/cells6040045

Niecknig H, Tug S, Reyes BD, et al., 2012. Role of reactive oxygen species in the regulation of HIF-1 by prolyl hydroxylase 2 under mild hypoxia. *Free Radic Res*, 46(6):705-717.
https://doi.org/10.3109/10715762.2012.669041

Olar A, Aldape KD, 2014. Using the molecular classification of glioblastoma to inform personalized treatment. *J Pathol*, 232(2):165-177.
https://doi.org/10.1002/path.4282

Omuro A, DeAngelis LM, 2013. Glioblastoma and other malignant gliomas: a clinical review. *JAMA*, 310(17):1842-1850.
https://doi.org/10.1001/jama.2013.280319

Peng PH, Lai JCY, Hsu KW, et al., 2020. Hypoxia-induced lncRNA RP11-390F4.3 promotes epithelial-mesenchymal transition (EMT) and metastasis through upregulating EMT regulators. *Cancer Lett*, 483:35-45.
https://doi.org/10.1016/j.canlet.2020.04.014

Perillo B, di Donato M, Pezone A, et al., 2020. ROS in cancer therapy: the bright side of the moon. *Exp Mol Med*, 52(2):192-203.
https://doi.org/10.1038/s12276-020-0384-2

Polyak K, Weinberg RA, 2009. Transitions between epithelial

and mesenchymal states: acquisition of malignant and stem cell traits. *Nat Rev Cancer*, 9(4):265-273. https://doi.org/10.1038/nrc2620

Quinlan CL, Orr AL, Perevoshchikova IV, et al., 2012. Mitochondrial complex II can generate reactive oxygen species at high rates in both the forward and reverse reactions. *J Biol Chem*, 287(32):27255-27264. https://doi.org/10.1074/jbc.M112.374629

Schieber M, Chandel NS, 2014. ROS function in redox signaling and oxidative stress. *Curr Biol*, 24(10):R453-R462. https://doi.org/10.1016/j.cub.2014.03.034

Schumacker PT, 2011. SIRT3 controls cancer metabolic reprogramming by regulating ROS and HIF. *Cancer Cell*, 19(3): 299-300. https://doi.org/10.1016/j.ccr.2011.03.001

Semenza GL, 1998. Hypoxia-inducible factor 1: master regulator of O_2 homeostasis. *Curr Opin Genet Dev*, 8(5):588-594. https://doi.org/10.1016/s0959-437x(98)80016-6

Semenza GL, 2014. Oxygen sensing, hypoxia-inducible factors, and disease pathophysiology. *Annu Rev Pathol Mech Dis*, 9:47-71. https://doi.org/10.1146/annurev-pathol-012513-104720

Spencer NY, Engelhardt JF, 2014. The basic biology of redoxosomes in cytokine-mediated signal transduction and implications for disease-specific therapies. *Biochemistry*, 53(10):1551-1564. https://doi.org/10.1021/bi401719r

Srivastava C, Irshad K, Dikshit B, et al., 2018. FAT1 modulates EMT and stemness genes expression in hypoxic glioblastoma. *Int J Cancer*, 142(4):805-812. https://doi.org/10.1002/ijc.31092

Subramanian A, Tamayo P, Mootha VK, et al., 2005. Gene set enrichment analysis: a knowledge-based approach for interpreting genome-wide expression profiles. *Proc Natl Acad Sci USA*, 102(43):15545-15550. https://doi.org/10.1073/pnas.0506580102

Sun B, Yu L, Xu C, et al., 2021. NAD(P)HX epimerase downregulation promotes tumor progression through ROS/HIF-1α signaling in hepatocellular carcinoma. *Cancer Sci*, 112(7):2753-2769. https://doi.org/10.1111/cas.14925

Takayama Y, Hattori N, Hamada H, et al., 2016. Inhibition of PAI-1 limits tumor angiogenesis regardless of angiogenic stimuli in malignant pleural mesothelioma. *Cancer Res*, 76(11):3285-3294. https://doi.org/10.1158/0008-5472.CAN-15-1796

Tang ZH, Zhang ZH, Lin QQ, et al., 2021. HIF-1α/BNIP3-mediated autophagy contributes to the luteinization of granulosa cells during the formation of corpus luteum. *Front Cell Dev Biol*, 8:619924. https://doi.org/10.3389/fcell.2020.619924

Teng F, Zhang JX, Chen Y, et al., 2021. LncRNA NKX2-1-AS1 promotes tumor progression and angiogenesis via upregulation of SERPINE1 expression and activation of the VEGFR-2 signaling pathway in gastric cancer. *Mol Oncol*, 15(4):1234-1255. https://doi.org/10.1002/1878-0261.12911

Thiery JP, Acloque H, Huang RYJ, et al., 2009. Epithelial-mesenchymal transitions in development and disease. *Cell*, 139(5):871-890. https://doi.org/10.1016/j.cell.2009.11.007

Tsai JH, Yang J, 2013. Epithelial-mesenchymal plasticity in carcinoma metastasis. *Genes Dev*, 27(20):2192-2206. https://doi.org/10.1101/gad.225334.113

Vordermark D, 2005. Significance of hypoxia in malignant glioma. Re: Evans et al. Hypoxia is important in the biology and aggression of human glial brain tumors. Clin Cancer Res 2004;10:8177-84. *Clin Cancer Res*, 11(10): 3966-3968. https://doi.org/10.1158/1078-0432.CCR-05-0097

Wang Q, Lu WJ, Yin T, et al., 2019. Calycosin suppresses TGF-β-induced epithelial-to-mesenchymal transition and migration by upregulating BATF2 to target PAI-1 via the Wnt and PI3K/Akt signaling pathways in colorectal cancer cells. *J Exp Clin Cancer Res*, 38:240. https://doi.org/10.1186/s13046-019-1243-7

Wang XW, Bustos MA, Zhang XQ, et al., 2020. Downregulation of the ubiquitin-E3 ligase RNF123 promotes upregulation of the NF-κB1 target SerpinE1 in aggressive glioblastoma tumors. *Cancers (Basel)*, 12(5):1081. https://doi.org/10.3390/cancers12051081

Wang ZL, Shi YP, Ying CT, et al., 2021. Hypoxia-induced PLOD1 overexpression contributes to the malignant phenotype of glioblastoma via NF-κB signaling. *Oncogene*, 40(8):1458-1475. https://doi.org/10.1038/s41388-020-01635-y

Watson J, 2013. Oxidants, antioxidants and the current incurability of metastatic cancers. *Open Biol*, 3(1):120144. https://doi.org/10.1098/rsob.120144

Weidemann A, Johnson RS, 2008. Biology of HIF-1α. *Cell Death Differ*, 15(4):621-627. https://doi.org/10.1038/cdd.2008.12

Willson JA, Arienti S, Sadiku P, et al., 2022. Neutrophil HIF-1α stabilization is augmented by mitochondrial ROS produced via the glycerol 3-phosphate shuttle. *Blood*, 139(2):281-286. https://doi.org/10.1182/blood.2021011010

Wilson WR, Hay MP, 2011. Targeting hypoxia in cancer therapy. *Nat Rev Cancer*, 11(6):393-410. https://doi.org/10.1038/nrc3064

Wu K, Mao YY, Chen Q, et al., 2021. Hypoxia-induced ROS promotes mitochondrial fission and cisplatin chemosensitivity via HIF-1α/Mff regulation in head and neck squamous cell carcinoma. *Cell Oncol (Dordr)*, 44(5):1167-1181. https://doi.org/10.1007/s13402-021-00629-6

Xia LM, Mo P, Huang WJ, et al., 2012. The TNF-α/ROS/HIF-1-induced upregulation of FoxMI expression promotes HCC proliferation and resistance to apoptosis. *Carcinogenesis*, 33(11):2250-2259. https://doi.org/10.1093/carcin/bgs249

Xu BD, Bai ZG, Yin J, et al., 2019. Global transcriptomic analysis identifies *SERPINE1* as a prognostic biomarker associated with epithelial-to-mesenchymal transition in gastric cancer. *PeerJ*, 7:e7091.

https://doi.org/10.7717/peerj.7091

Xu YQ, Chen WC, Liang J, et al., 2021. The miR-1185-2-3p-GOLPH3L pathway promotes glucose metabolism in breast cancer by stabilizing p53-induced SERPINE1. *J Exp Clin Cancer Res*, 40:47. https://doi.org/10.1186/s13046-020-01767-9

Yang J, Antin P, Berx G, et al., 2020. Guidelines and definitions for research on epithelial-mesenchymal transition. *Nat Rev Mol Cell Biol*, 21(6):341-352. https://doi.org/10.1038/s41580-020-0237-9

Yang JL, Ma Q, Zhang MM, et al., 2021. LncRNA CYTOR drives L-OHP resistance and facilitates the epithelial-mesenchymal transition of colon carcinoma cells via modulating miR-378a-5p/SERPINE1. *Cell Cycle*, 20(14): 1415-1430. https://doi.org/10.1080/15384101.2021.1934626

Yang Y, Zhang GM, Guo FZ, et al., 2020. Mitochondrial UQCC3 modulates hypoxia adaptation by orchestrating OXPHOS and glycolysis in hepatocellular carcinoma. *Cell Rep*, 33(5):108340. https://doi.org/10.1016/j.celrep.2020.108340

Yu LM, Zhang WH, Han XX, et al., 2019. Hypoxia-induced ROS contribute to myoblast pyroptosis during obstructive sleep apnea via the NF-κB/HIF-1α signaling pathway. *Oxid Med Cell Longev*, 2019:4596368. https://doi.org/10.1155/2019/4596368

Zhang W, Zhang YW, Zhou WS, et al., 2021. PlGF knockdown attenuates hypoxia-induced stimulation of cell proliferation and glycolysis of lung adenocarcinoma through inhibiting Wnt/β-catenin pathway. *Cancer Cell Int*, 21:18. https://doi.org/10.1186/s12935-020-01714-w

Zhang YS, Jin GS, Zhang JW, et al., 2018. Overexpression of STAT1 suppresses angiogenesis under hypoxia by regulating VEGF-A in human glioma cells. *Biomed Pharmacother*, 104:566-575. https://doi.org/10.1016/j.biopha.2018.05.079

Zhao Q, Zhang LW, He QF, et al., 2023. Targeting *TRMT5* suppresses hepatocellular carcinoma progression via inhibiting the HIF-1α pathways. *J Zhejiang Univ-Sci B (Biomed & Biotechnol)*, 24(1):50-63. https://doi.org/10.1631/jzus.B2200224

Zheng H, Kang Y, 2014. Multilayer control of the EMT master regulators. *Oncogene*, 33(14):1755-1763. https://doi.org/10.1038/onc.2013.128

Zong SQ, Tang YF, Li W, et al., 2020. A Chinese herbal formula suppresses colorectal cancer migration and vasculogenic mimicry through ROS/HIF-1α/MMP2 pathway in hypoxic microenvironment. *Front Pharmacol*, 11:705. https://doi.org/10.3389/fphar.2020.00705

Supplementary information

Tables S1–S3; Figs. S1–S4